# Supporting Information

## Investigating Miscibility and Lithium Ion Transport in Blends of Poly(ethylene oxide) with a Polyanion Containing Precisely-Spaced Delocalized Charges

Nam Nguyen, Michael Patrick Blatt, Kyoungmin Kim, Daniel T. Hallinan Jr.*, and Justin G. Kennemur*

## Table of Contents:

## Materials:

Acetonitrile (MeCN, ≥ 99.9% anhydrous), hexane (≥ 98.5%, ACS reagent), chloroform (≥ 99.9%, HPLC Plus), benzaldehyde (≥ 99.0%, ReagentPlus), titanium (IV) chloride (≥ 99.9%, trace metal basis), Grubbs 1st generation catalyst (G1, Umicore M102, 97%), Hoveyda-Grubbs 2nd generation catalyst (HG2, M720, 97.0%), ethyl vinyl ether (EVE, 99.0%), *o*-xylene (≥ 98%, ACS reagent), triethylamine (99%), tributylamine (≥98.5%, ACS reagent), 4-(dimethylamino)pyridine (DMAP ≥99%), benzene (≥99.0%, ACS reagent), sulfuric acid (95.0-98.0%, ACS reagent), oxalyl chloride (≥99%, ACS reagent) were purchased from Sigma-Aldrich and used as received. Allyltrimethylsilane (96.0%), *p*-toluenesulfonyl hydrazide (95.0%), trifluoromethanesulfonamide (98 %) were purchased from Oakwood Chemicals and used as received. Hydrochloric acid (36.5 – 38%) was obtained from VWR and used as received. Nitromethane (99.0%, Oakwood Chemicals) was dried by distillation under $CaCl_2$. Anhydrous lithium hydroxide (99.995%, trace metal basis) was used as received from Beantown chemical. DMSO-$d_6$ was purchased from Alfa Aesar and stored under 4Å molecular sieves. Dry toluene, dichloromethane, dimethylformamide (DMF) were obtained from an SG Waters glass contour solvent purification system by passage

through columns packed with neutral alumina followed by a 2 μm filter.

## Characterization methods:

$^{1}$H NMR, $^{19}$F NMR and $^{13}$C NMR experiments were performed on a Bruker Avance 600, 375 and 150 MHz Spectrometer, respectively. Thermogravimetric analysis (TGA) was performed on a TA instruments SDT Q600 under argon with the flow rate of 10 °C min$^{-1}$. Number average molar mass ($M_n$) and as dispersity (Đ) was determined on an Agilent-Wyatt combination triple detection size exclusion chromatograph (SEC) instrument with THF mobile phase at 25 °C. The Wyatt triple-detection system was comprised of a miniDawn TREOS 3-angle light scattering detector, a Viscostar II differential viscometer, and an Optilab TrEX refractive index detector. Conventional column calibration was performed with polystyrene standards ranging from 2 to 2000 kDa (10 total points). Differential scanning calorimetry (DSC) experiments were performed on a TA Instruments Model Q100 with a heating rate of 30 °C min$^{-1}$ under nitrogen flow (50 mL min$^{-1}$).. Lyophilization was performed on Labconco FreeZone 4.5L (-104 °C). Samples were fully dried in a VWR Vacuum Oven (Model No. 6291) at 130 °C and 0.092 mTorr. pH was determined with a VWR model SB20 with a sympHony Ag/AgCl pH electrode. Attenuated total reflectance infrared spectroscopy (ATR-IR) was performed on a Bruker Alpha FTIR spectrometer with a Platinum ATR quickSnap sampling module (single reflection diamond crystal).

## Synthetic procedure*:*

The parent polymer (p5Ph), was produced from ROMP of 4-phenylcyclopentene using HG2 catalyst at a molar ratio of [4PCP]:[HG2] = 208 in THF at – 15 °C and was quantitatively hydrogenated using *p*-toluenesulfonyl hydrazide as described previously.[24, 25] Analysis of *p*5Ph by SEC determined $M_n$ = 13 kg mol$^{-1}$ and Đ = 1.57 (Figure S2). Sulfonation of p5Ph to the phenylsulfonic acid analog (p5PhS-H) was performed by reacting in concentrated sulfuric acid at 90 °C for 48 hrs as described previously. The percent sulfonation (94%) was determined through

titration of an aqueous solution of *p*5PhS-H (sulfonic acid form) at known mass with an analytical standard of 9.48 mM NaOH (aq) and analysis of the equivalence point where the maximum change in pH resulted as a function of NaOH titration. The bulk *p*5PhS-H sample was then converted to p5PhS-Na (neutralized sodium form) through excess addition of NaOH (aq) followed by dialysis within SnakeSkin tubing (ThermoScientific, 3.5 kDa cutoff) to remove excess salt

**Conversion phenylsulfonate sodium salt to of phenylsulfonyl chloride.**

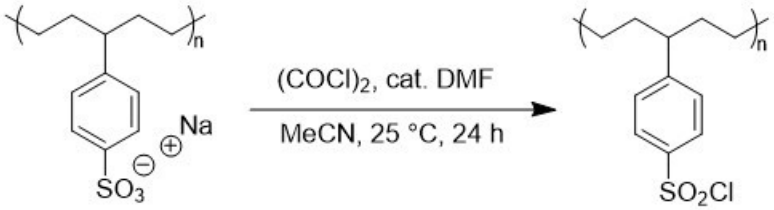


**Scheme 1.** Conversion of phenylsulfonate sodium salt to phenylsulfonyl chloride of *p*5Ph

In a 250 mL round bottom flask (rbf), the generation of Vilsmeier-Haack reagent was done by dissolving a catalytic amount of DMF in 120 mL of anhydrous acetonitrile. Oxalyl chloride (0.75 mL, 2 mol eq) was added dropwise slowly into the solution and the carbon monoxide produced was vented through tubing attached to an oil bubbler. Following complete addition, the reaction was stirred at 25 °C for 4 h. The *p*5PhS-Na (1.12 g, 4.7 mmol of sulfonate) was added to the rbf and the reaction was stirred for 24 h under an Ar balloon at 25 °C. Here we note that full dissolution of the p5PhS-Na did not occur and the reaction was successful heterogeneously. Workup was performed by separating the polymeric solids by centrifugation and washing the collected polymer with acetonitrile (3 x 50 mL) to remove impurities. The phenylsulfonyl chloride derivative (*p*5PhS-Cl) was immediately dried in a vacuum oven at 65 °C for 16 h. Due to the reactivity of this derivative with moisture and other nucleophiles it was used immediately in the next step.

**Conversion of phenylsulfonyl chloride to phenylsulfonyl(trifluoromethylsulfonyl)imide lithium salt.**


**Scheme 2.** Conversion of phenylsulfonyl chlorie to phenyl sulfonyl(trifluoromethylsulfonyl)imide lithium salt of *p*5Ph

In a 250 mL rbf, *p*5PhS-Cl (1.08 g, 4.39 mmol sulfonyl chloride based on full conversion) was added, and the flask was purged with Ar for 15 min. A solution of triethylamine (1.67 mL, 2.5 mol eq), $CF_3SO_2NH_2$ (1.43 g, 2 mol eq) and catalytic amount of DMAP were dissolved in 100 mL of anhydrous acetonitrile. The solution was added into the flask, and the reaction was stirred for 24 h under Ar at 25 °C. The mixture was centrifuged and filtered under vacuum to remove triethylammmonium salt. The filtrate was collected and volatiles were removed by rotary evaporation at 40 °C. The remaining residue was dissolved successfully in methanol (60 mL) and subsequently added to SnakeSkin tubing and dialyzed within a 4 L beaker containing 0.5 M aqueous solution of HCl. The remaining impurities of DMAP and triethylamine were slowly removed by dialysis which was monitored by $^1$H NMR. Replacement of the 0.5 M HCl (aq) was performed several times until the impurities were completely removed. In order to neutralize the amine to the imide lithium salt, the polymer was further dialyzed in 0.2 M aqueous solution of LiOH for 24 h. A final dialysis within deionized water was performed until the pH of the outer solution remained constant (~7.5), indicating that excess LiOH was no longer dialyzing from within the tubing. The pH within the dialysis tubing was then measured and determined to be 5.3.

The polymer was lyophilized, collected, and finally dried in a vacuum oven at 160 °C for 24 h to obtain 0.96 g of *p*5PhTFSI-Li (55.6 % yield based on starting amount of *p*5PhS-Na). $^{1}$H NMR (600MHz, $CDCl_3$): $\delta$ (ppm) 7.71 – 7.00 (m, 4H, aryl H), 2.43 – 2.21 (br, 1H, $CH_2$-C*H*-$CH_2$), 1.60 – 1.15 (br, 4H, CH-C*H*$_2$-$CH_2$), 1.11 – 0.59 (br, 4H, $CH_2$-C*H*$_2$-$CH_2$). $^{19}$F NMR (375 MHz, DMSO-$d_6$) $\delta$ (ppm): -77.9. $^{13}$C NMR (150 MHz, DMSO-$d_6$): 149.6, 142.9, 127.7, 126.5, 123.7, 121.6, 119.4, 117.3, 45.9, 36.7, 27.8. IR ($cm^{-1}$) :3490, 2910, 2840, 1600 1320, 1280, 1160, 1067, 790, 745

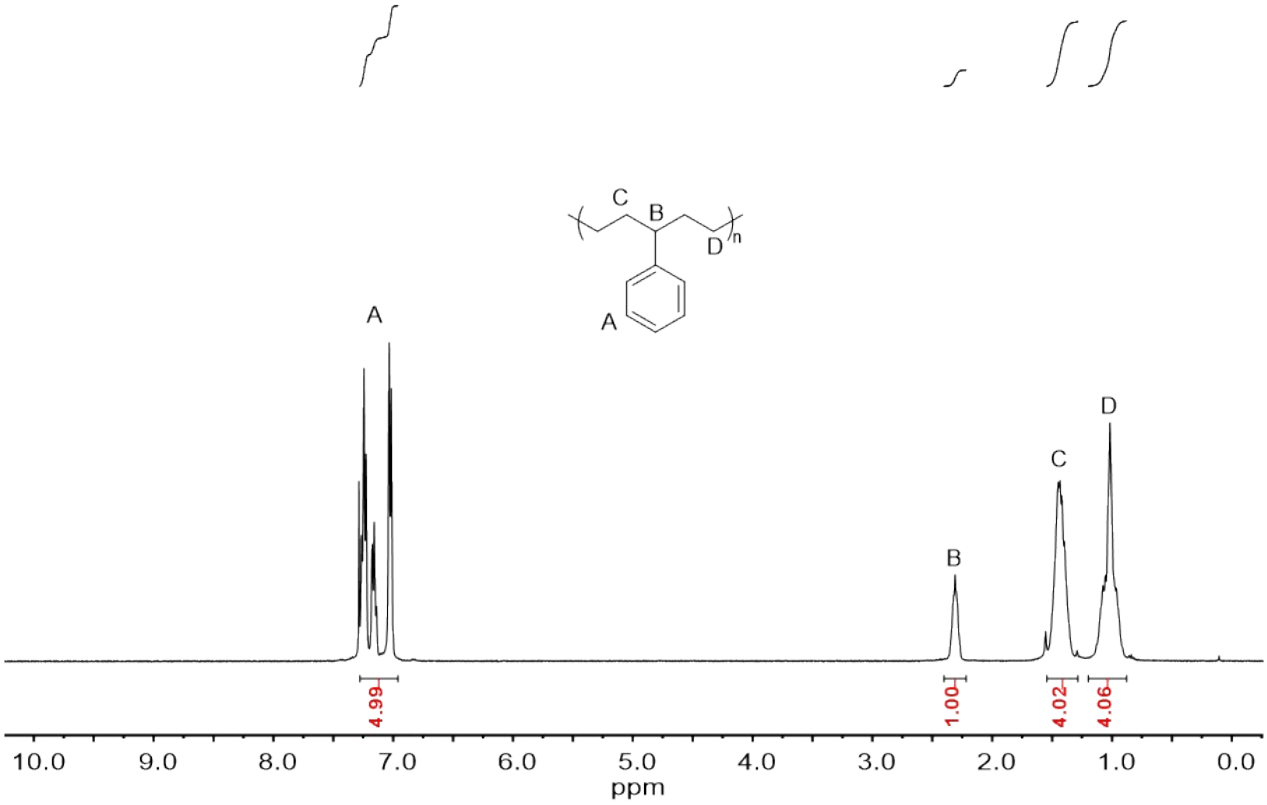


**Figure S1**.$^{1}$H NMR of parent *p*5Ph. Solvent: $CDCl_3$ (600MHz, 25 °C)

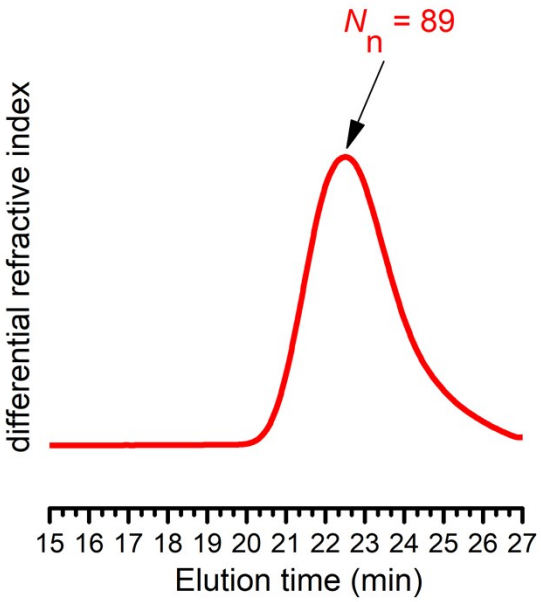


**Figure S2**. SEC differential refractive index as a function of elution time (THF mobile phase, 25 °C) of parent *p*5Ph. $M_n$ = 13.0 kg mol$^{-1}$ and $Đ$ = 1.57 determined by conventional column calibration.

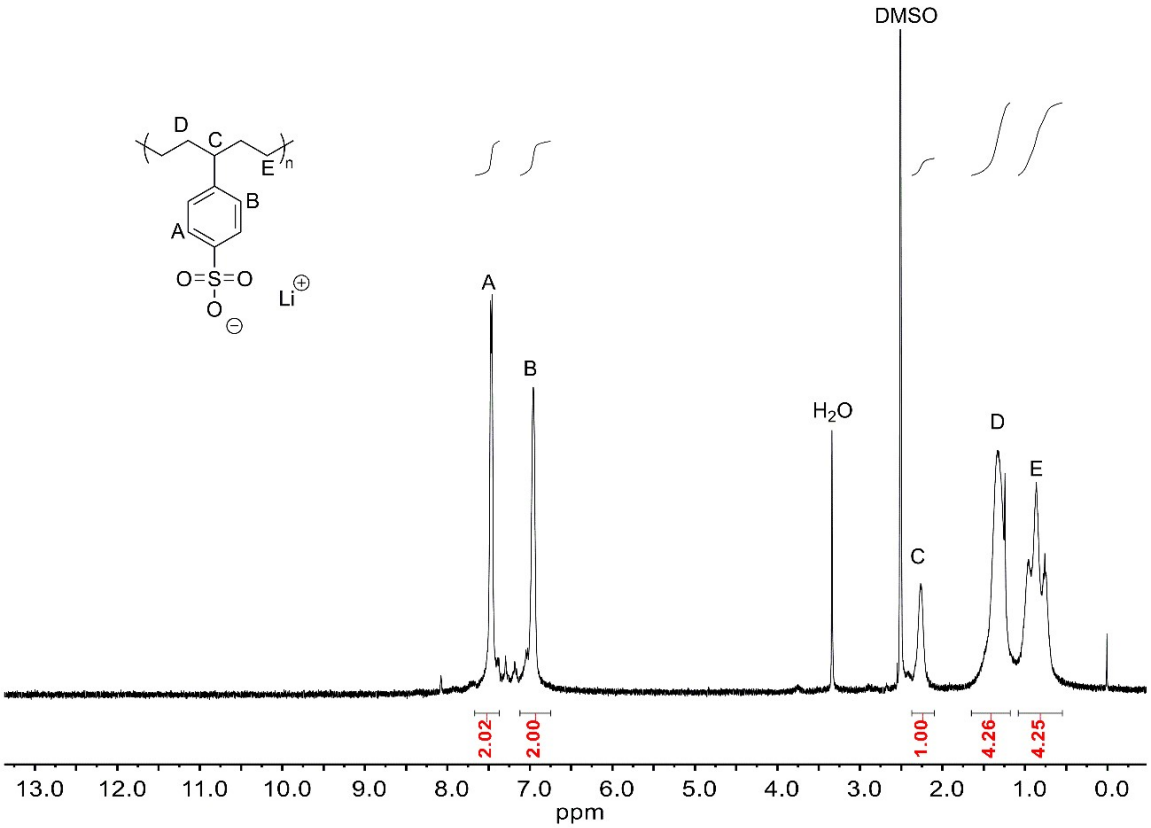


**Figure S3**. $^{1}$H NMR (600 MHz, DMSO-$d_6$, 25 °C) of *p*5PhS-Li.

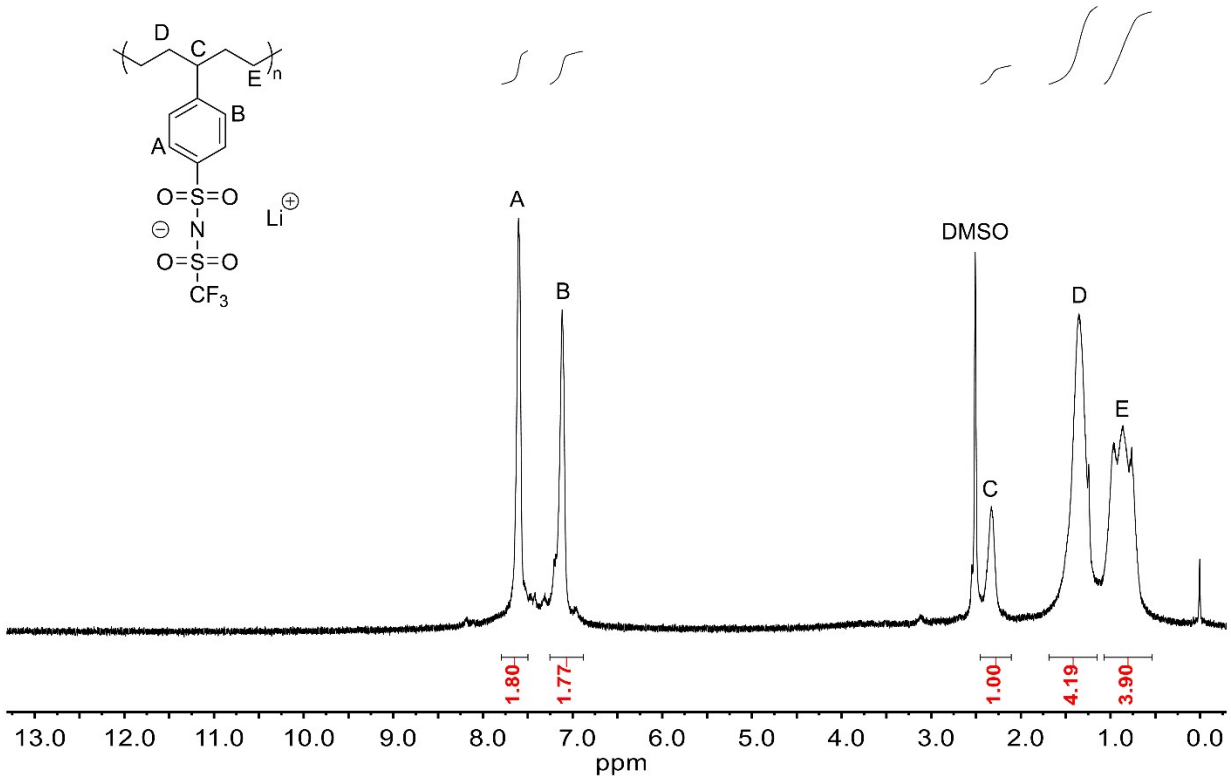


**Figure S4.** $^{1}$H NMR (600 MHz, DMSO-$d_6$, 25 °C) of *p*5PhTFSI-Li.

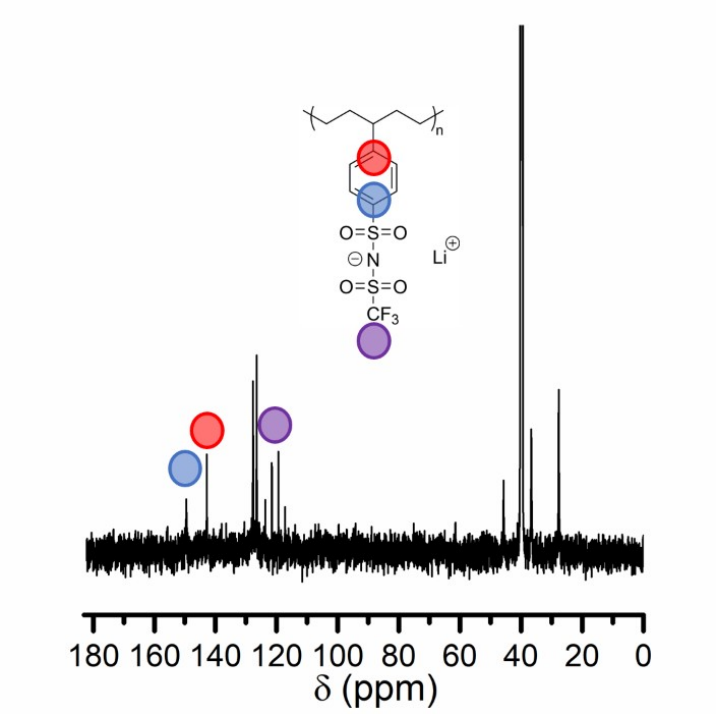


**Figure S5.** $^{13}$C NMR (150 MHz, DMSO-$d_6$, 25 °C) of *p*5PhTFSI-Li. Colored circles represent key signals discussed in main manuscript and annotated on the provided structure.

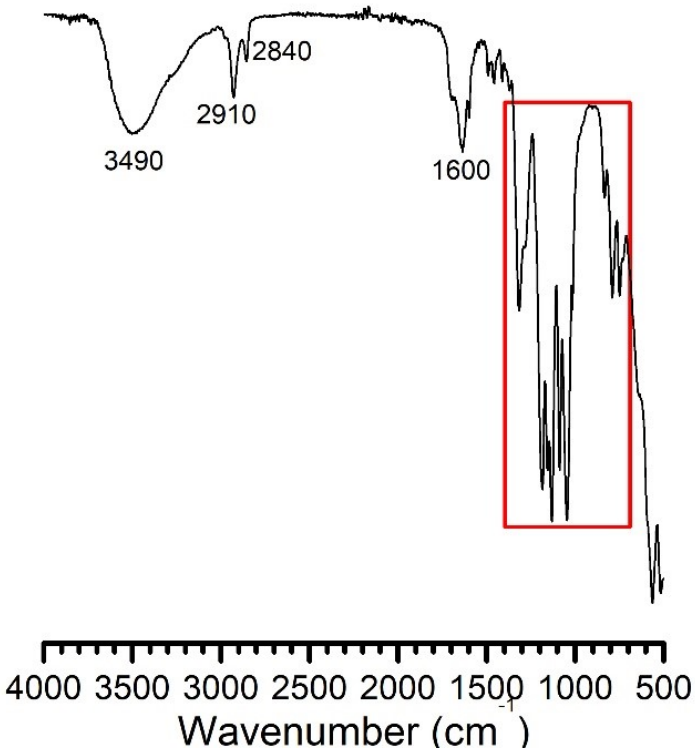


**Figure S6.** ATR-IR spectrum of *p*5PhTFSI-Li. Red box represents key vibrations discussed in main manuscript.

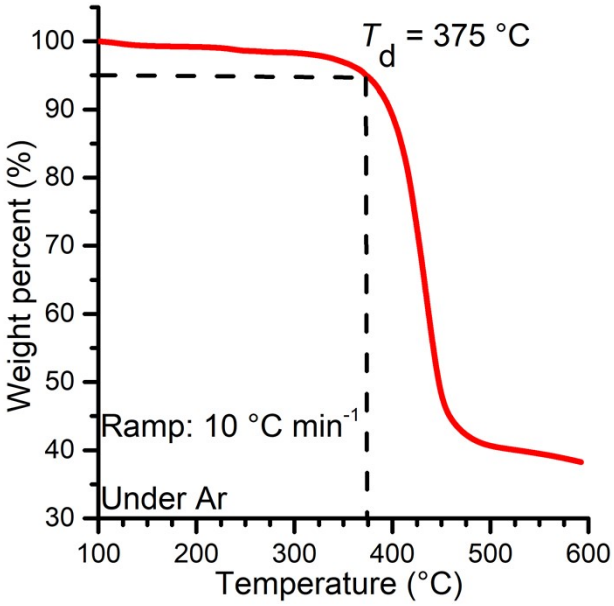


**Figure S7**. TGA of *p*5PhTFSI-Li. The decomposition temperature ($T_d$ = 375 °C) was determined at 5 % mass loss (dashed line) (Heating rate: 10 °C min$^{-1}$ under Argon).

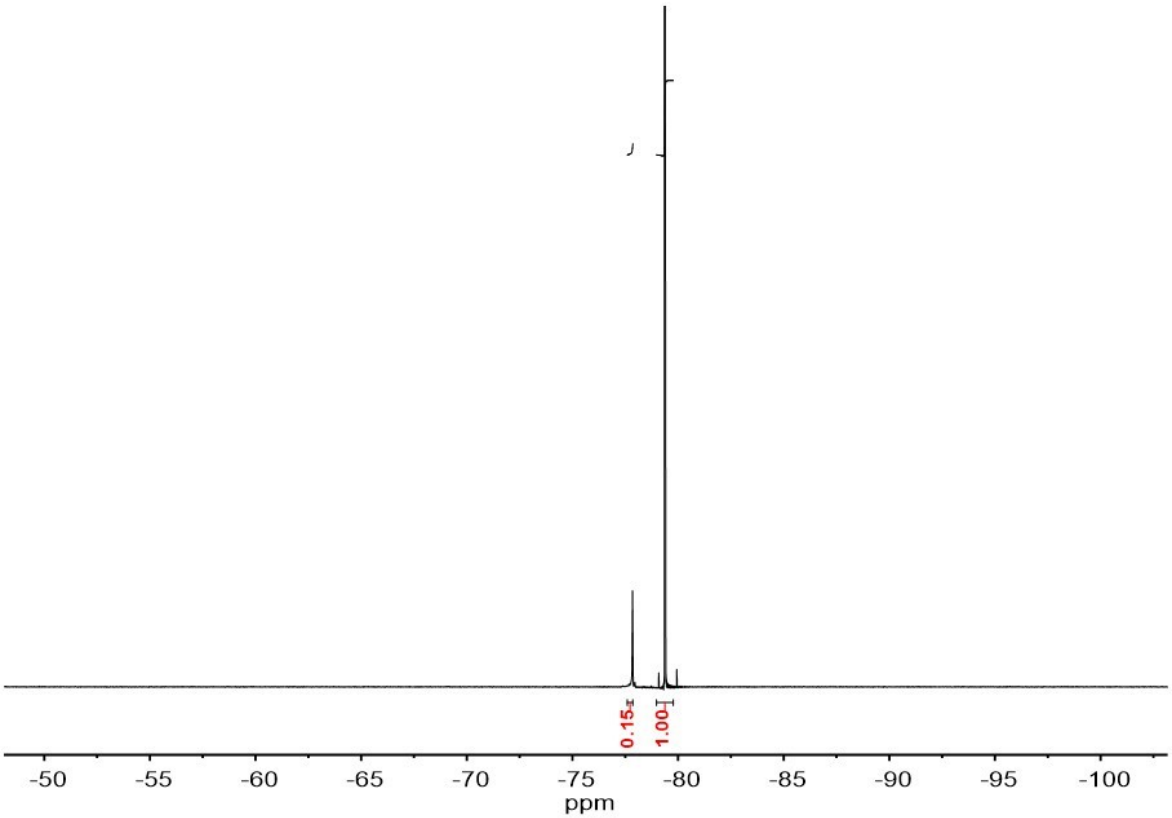


**Figure S8**. $^{19}$F NMR (375 MHz, DMSO-$d_6$, 25 °C) of *p*5PhTFSI-Li (–77.9 ppm) with an internal standard of $CF_3SO_2NH_2$ (–79.4 ppm).

**Methods and Calculations to Determine %TFSI functionalization of *p*5PhTFSI-Li**

In a 4 mL vial, an internal standard of $CF_3SO_2NH_2$ (8.3 mg) was added along with *p*5PhTFSI-Li (3.6 mg) and dissolved in 500 µL of DMSO-$d_6$. $^{19}F$ NMR was performed and the spectrum was analyzed by integrative comparison of the polymer fluorine signal with that of the internal standard.

Calculation:

Moles of internal standard (8.3 mg);

$$mole_{CF_3SO_2NH_2} = \frac{0.0083}{149.09} = 5.56 \times 10^{-5}\ (mole)$$

The integration value of the fluorine signal for *p*5PhTFSI-Li (0.15) and $CF_3SO_2NH_2$ (integration set at 1.00) can be used to determine the mole content of TFSI in the polymer

$$mole_{5PhTFSI-Li} = 5.56 \times 10^{-5} \times 0.15 = 8.35 \times 10^{-6} (mole)$$

The maximum theoretical moles of TFSI if all of the polymer's repeating units were functionalized is:

$$Theoretical\ mole_{5PhTFSI-Li} = \frac{0.0036}{363.3} = 9.9 \times 10^{-6}\ (mole)$$

Actual TFSI content can be calculate as below:

$$\%\ TFSI = \frac{Actual\ mole_{5PhTFSI-Li}}{Theoretical\ mole_{5PhTFSI-Li}} = \frac{8.35 * 10^{-6}}{9.9 \times 10^{-6}} \times 100 = 84.3$$

Therefore, ~84% of the repeating units contain a TFSI functionality based on this treatment. Since the % sulfonation of the *p*5Ph parent polymer was determined to be 94%, the efficiency of the conversion from sulfonate sodium salt to trifluorosulfonamide was ~90%. Here we note that these values are best approximations due to the fact that the repeating unit molar mass varies based on the actual functionality of that unit.

**Figure S9.** Sample appearance of *p*5PhTFSI-Li

**Table S1**. Electrochemical characterization blend composition and casting environment

| Sample | Weight fraction of PEO | Cation to oxygen molar ratio ($[Li^+]/[EO]$) | Solvent MeCN:$H_2O$ (Volume Ratio) | Casting Atmosphere |
|---|---|---|---|---|
| PEO | 1 | 0 | 1:0 | Argon |
| $EO_{0.90}PhTFSI_{0.10}$ | 0.9 | 0.013 | 1:0 | Argon |
| $EO_{0.80}PhTFSI_{0.20}$ | 0.8 | 0.031 | 1:0 | Argon |
| $EO_{0.70}PhTFSI_{0.30}$ | 0.7 | 0.051 | 1:0 | Argon |
| $EO_{0.58}PhTFSI_{0.42}$ | 0.58 | 0.087 | 80:20 | Air |
| $EO_{0.50}PhTFSI_{0.50}$ | 0.5 | 0.13 | 80:20 | Air |
| $EO_{0.30}PhTFSI_{0.70}$ | 0.3 | 0.29 | 80:20 | Air |
| $EO_{0.10}PhTFSI_{0.90}$ | 0.1 | 1.1 | 80:20 | Air |

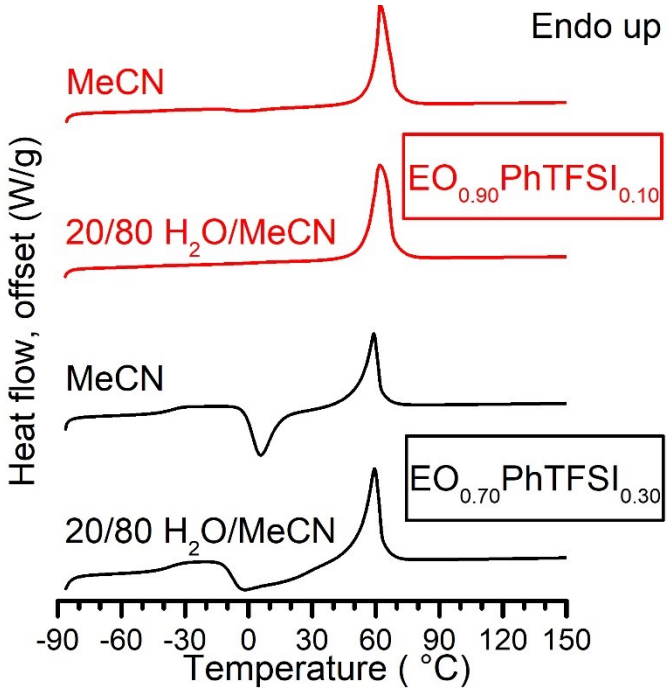


**Figure S10**. Stacked DSC thermograms of $EO_{0.90}PhTFSI_{0.10}$ and $EO_{0.70}PhTFSI_{0.30}$ blends casted with pure acetonitrile (MeCN) and mixture of 80/20 (v/v) of MeCN/$H_2O$. (Ramp = 30 °C $min^{-1}$, 3rd heating, endo up)

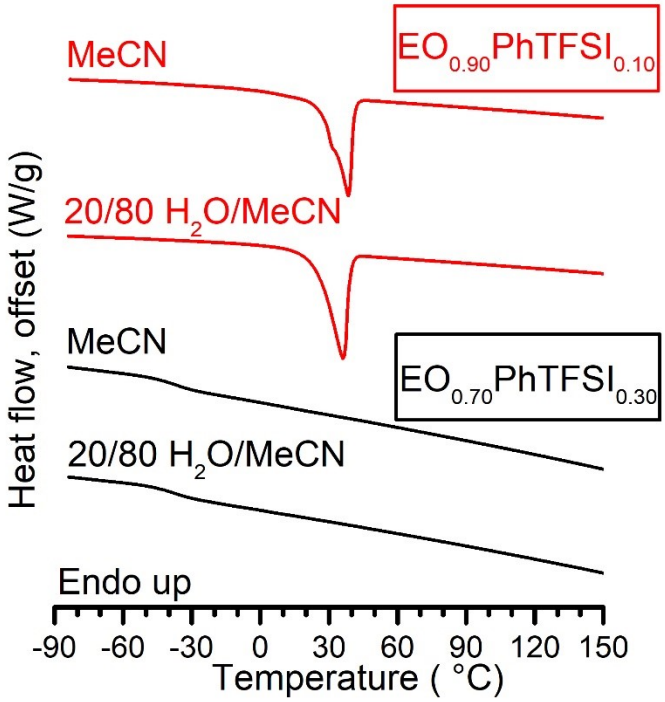


**Figure S11.** Stacked DSC thermograms of $EO_{0.90}PhTFSI_{0.10}$ and $EO_{0.70}PhTFSI_{0.30}$ blends casted with pure acetonitrile (MeCN) and mixture of 80/20 (v/v) of MeCN/$H_2O$. (Ramp = 100 °C $min^{-1}$, 2nd cooling, endo up)

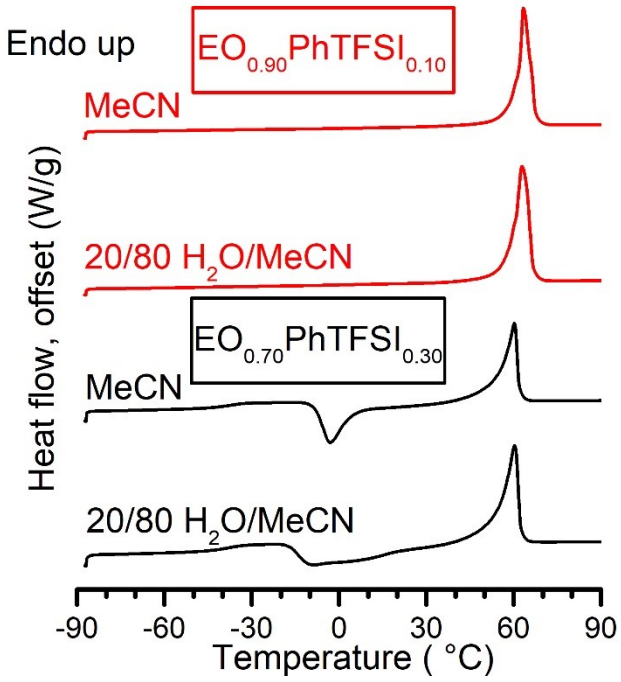


**Figure S12.** Stacked DSC thermograms of $EO_{0.90}PhTFSI_{0.10}$ and $EO_{0.70}PhTFSI_{0.30}$ blends casted with pure acetonitrile (MeCN) and mixture of 80/20 (v/v) of MeCN/$H_2O$. (Ramp = 10 °C $min^{-1}$, 3rd heating, endo up)

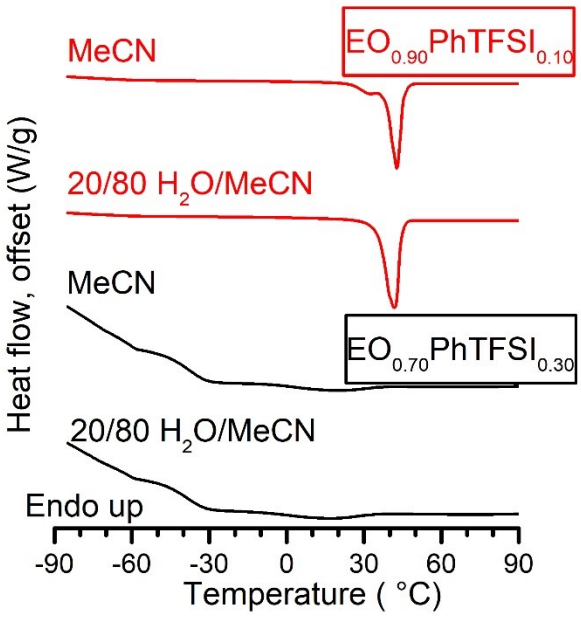


**Figure S13.** Stacked DSC thermograms of $EO_{0.90}PhTFSI_{0.10}$ and $EO_{0.70}PhTFSI_{0.30}$ blends casted with pure acetonitrile (MeCN) and mixture of 80/20 (v/v) of MeCN/$H_2O$. (Ramp = 10 °C $min^{-1}$, 2nd cooling, endo up)

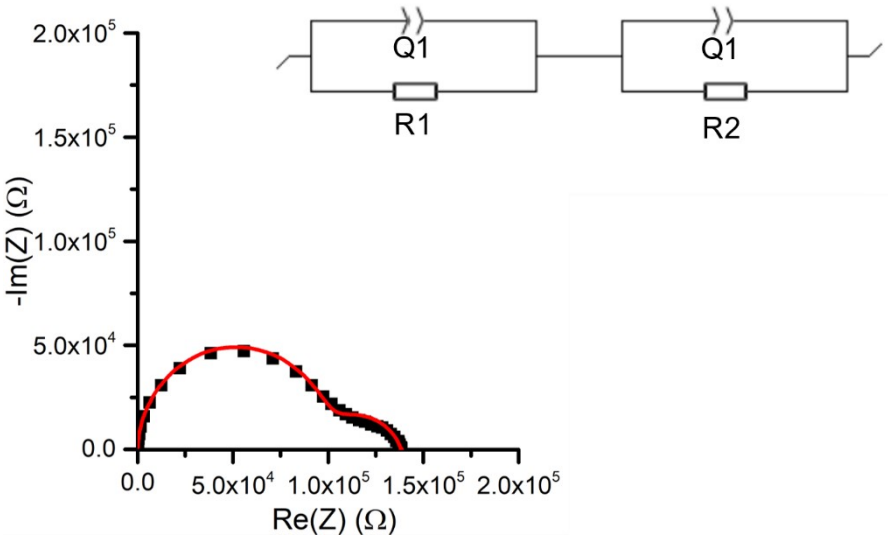


**Figure S14.** Nyquist plot For $EO_{0.90}PhTFSI_{0.10}$ with EIS data (Black Squares) and fitted equivalent circuit (red line) at 70 °C. Cell thickness =270 µm, Electrolyte Area = 31.7 $mm^2$. Q corresponds to a constant phase element capacitor while R corresponds to a resistor. $R_1$ was taken to be the bulk electrolyte resistance.

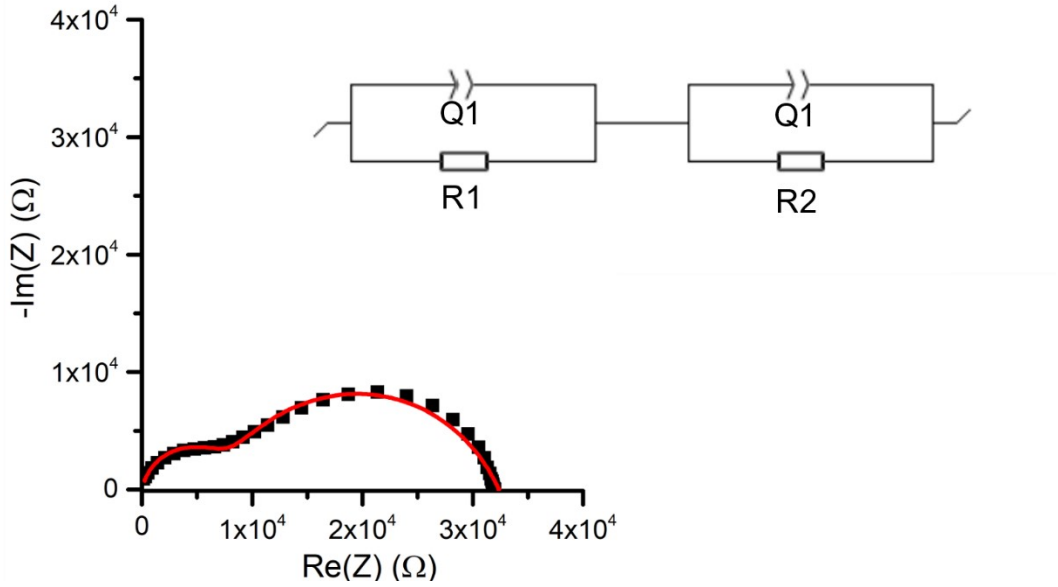


**Figure S15.** Nyquist plot For $EO_{0.70}PhTFSI_{0.30}$ with EIS data (Black Squares) and fitted equivalent circuit (red line) at 70 °C. Cell thickness = 167 µm, Electrolyte Area = 31.7 $mm^2$. Q corresponds to a constant phase element capacitor while R corresponds to a resistor. $R_1$ was taken to be the bulk electrolyte resistance.

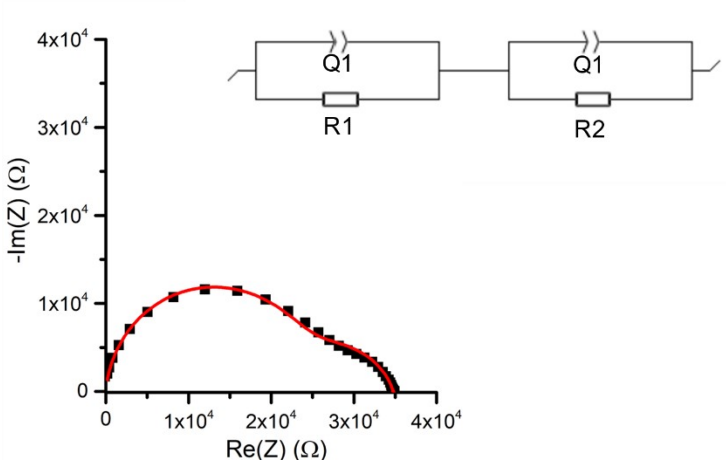


**Figure S16.** Nyquist plot For $EO_{0.58}PhTFSI_{0.52}$ with EIS data (Black Squares) and fitted equivalent circuit (red line) at 70 °C. Cell thickness = 157 µm, Electrolyte Area = 31.7 $mm^2$. Q corresponds to a constant phase element capacitor while R corresponds to a resistor. $R_1$ was taken to be the bulk electrolyte resistance.

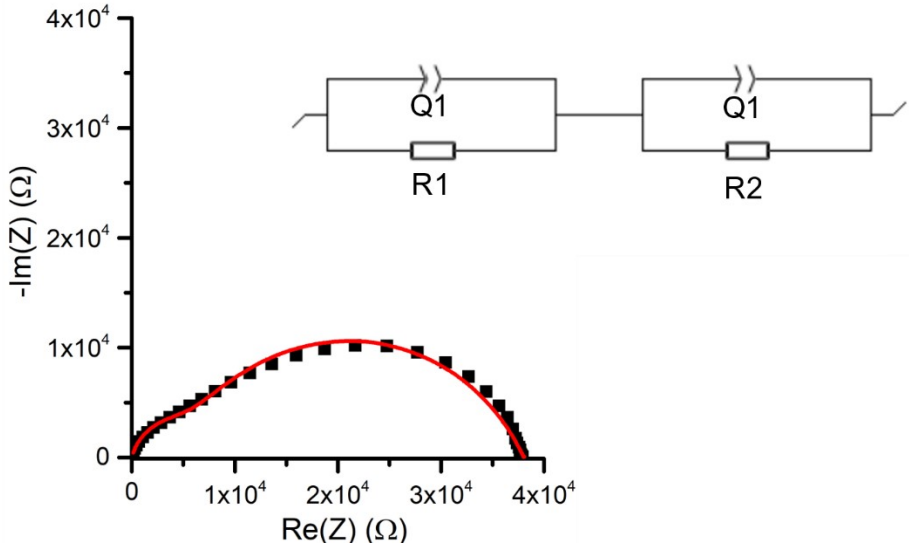


**Figure S17.** Nyquist plot For $EO_{0.50}PhTFSI_{0.50}$ with EIS data (Black Squares) and fitted equivalent circuit (red line) at 70 °C. Cell thickness =165 µm, Electrolyte Area = 31.7 $mm^2$. Q corresponds to a constant phase element capacitor while R corresponds to a resistor. $R_1$ was taken to be the bulk electrolyte resistance.

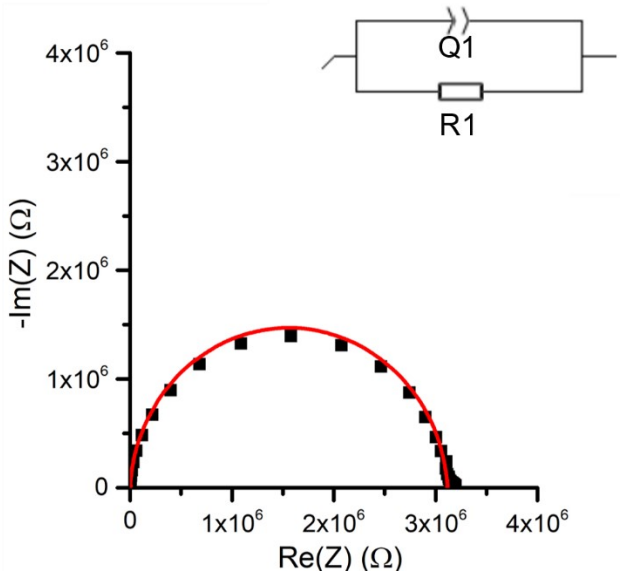


**Figure S18.** Nyquist plot For $EO_{0.30}PhTFSI_{0.70}$ with EIS data (Black Squares) and fitted equivalent circuit (red line) at 70 °C. Cell thickness = 421 µm, Electrolyte Area = 31.7 $mm^2$. Q corresponds to a constant phase element capacitor while R corresponds to resistor. $R_1$ was taken to be the bulk electrolyte resistance.

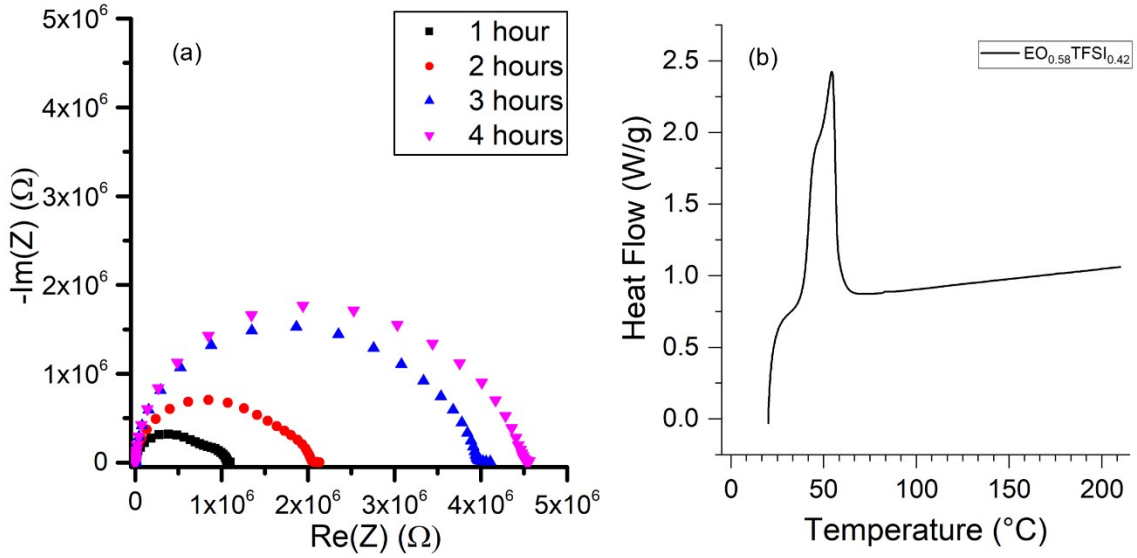


**Figure S19.** (a) Nyquist plot for repeated EIS measurements of $EO_{0.58}PhTFSI_{0.42}$ after 1,2,3 and 4 hours at 40 °C. The cell was first heated to 60 °C and allowed to cool for one hour prior to the first EIS measurement. Isothermal measurements were taken every hour thereafter. Cell thickness = 157 µm, electrolyte area = 31.7 $mm^2$. (b) DSC Thermogram of $EO_{0.58}PhTFSI_{0.42}$ after 12 hours of room temperature, isothermal crystallization. Ramp rate: 10 °C $min^{-1}$, endo up.

It should be noted that only one semicircle was observed in the Nyquist plot of $EO_{0.70}TFSI_{0.30}$ as can be seen in the Figure S18. As such, correction for electrode/electrolyte interfacial resistance (as represented by the diameter of the second semi-circle in Figures S14-S17) was not possible for $EO_{0.70}TFSI_{0.30}$. Thus, correcting the potentiostatic polarization method for electrode/electrolyte interfacial resistance at this composition was not possible. To determine if $EO_{0.70}TFSI_{0.30}$ was likely to be a single ion conductor, calculations were completed without this correction for each composition and good agreement between the methods was found, as can be seen by comparing Figure S20 and Figure 8 in the manuscript. $EO_{0.70}TFSI_{0.30}$ showed a cationic transference number of unity within one standard deviation at 60 °C and 90 °C.

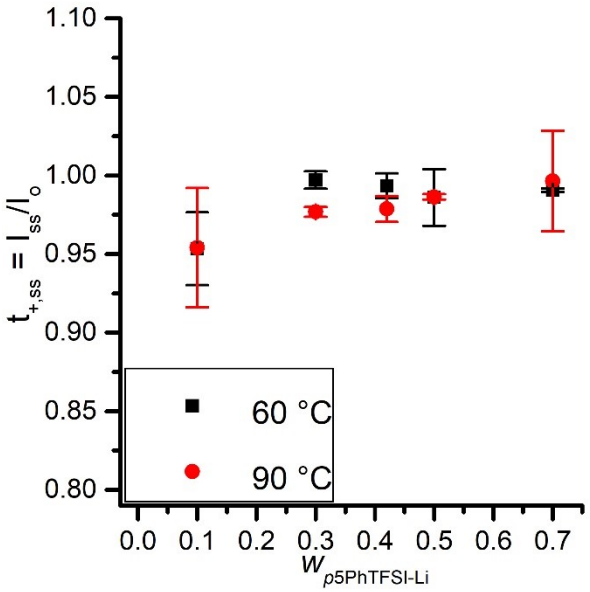


**Figure S20.** Transference number calculated without interfacial resistance correction of $EO_xPhTFSI_y$ at 60 °C and 90 °C. Error bars represent one standard deviation of 3 repeat measurements on at least 2 cells.

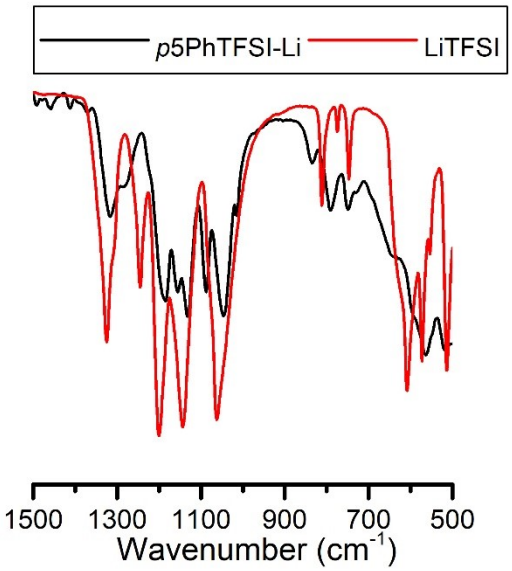


**Figure S21**. Overlay ATR-IR spectrum of *p*5PhTFSI-Li (black) and LiTFSI salt (red). The spectrum is shown between 1500 and 500 $cm^{-1}$ in order to observe similarity in molecular vibrations from the trifluoromethylsulfonyl imide functional group.

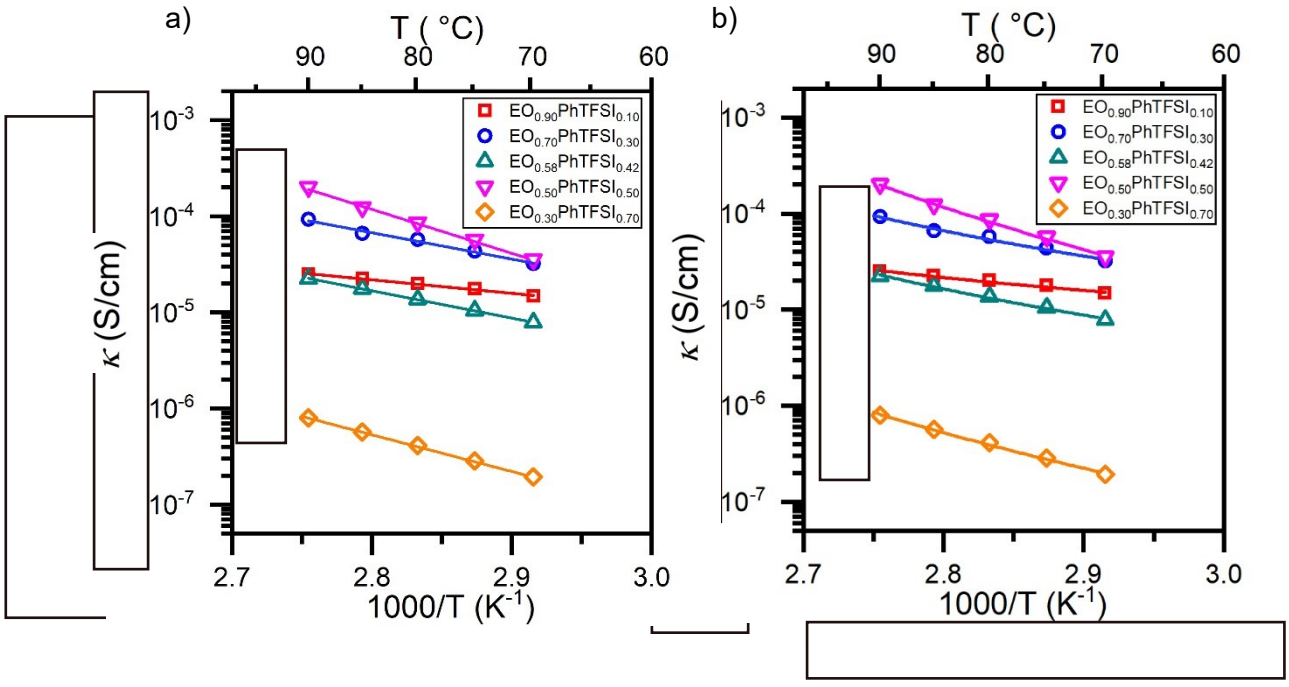

**Figure S22.** (a) Arrhenius model fit for the conductivity of $EO_xPhTFSI_y$ blends from 70 – 90 °C (b) Vogel-Fulcher-Tammann Model Fit for the conductivity of $EO_xPhTFSI_y$ blends from 70 – 90 °C.

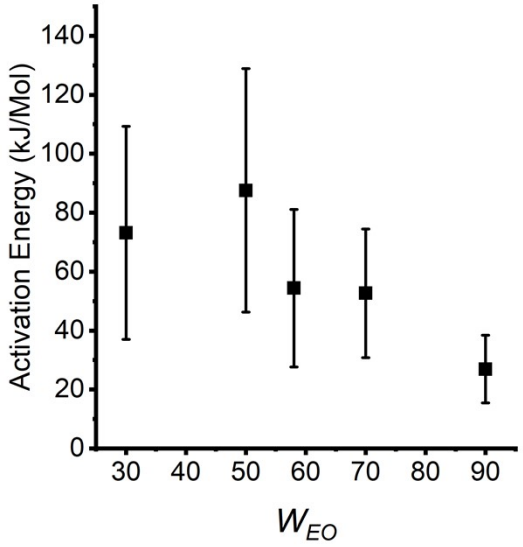


**Figure S23.** Composition dependence of ionic conductivity activation energy as predicted by to the Arrhenius temperature model of $EO_xPhTFSI_y$ blends. Each composition was fit from 70 – 90 °C with $R^2 > 0.99$ for all compositions. Error bars represent a 68.3% confidence interval.

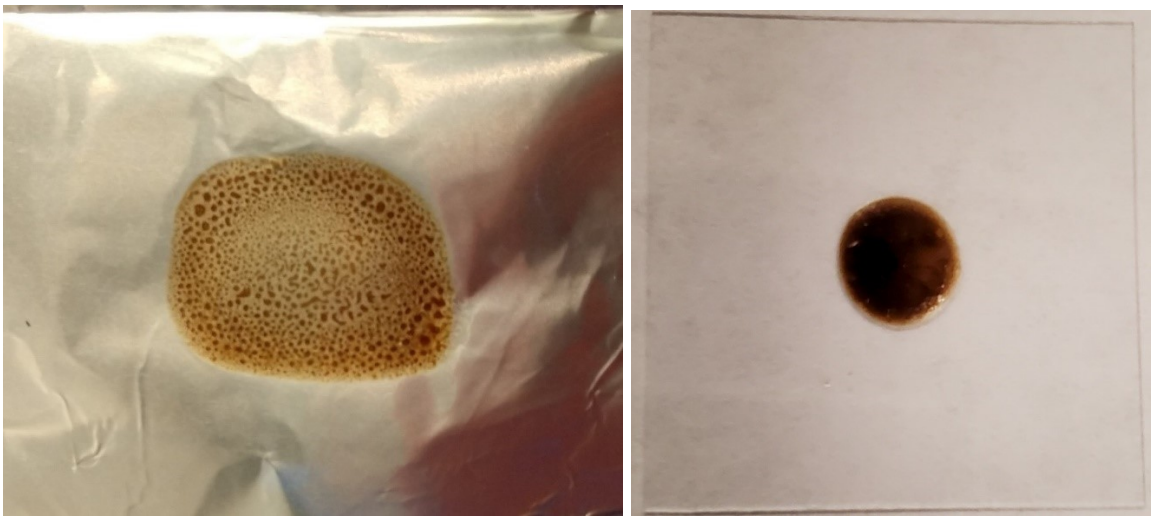

**Figure S24.** Photograph of $EO_{90}PhTFSI_{10}$ at 25 °C (left) and $EO_{80}PhTFSI_{20}$ (right) following casting and drying on aluminum foil (left) and a glass slide (right).

**Table S2.** Arrhenius equation fitting parameters of $EO_xPhTFSI_y$ blends. Each composition was fit from 70 °C to 90 °C and $R^2 > 0.99$ for all compositions.

| Sample | $\kappa_0$ (S/cm) | $E_a$ (kJ/mol) | $R^2$ |
|---|---|---|---|
| $EO_{0.90}PhTFSI_{0.10}$ | $1.89 \times 10^{-1}$ | $26.9 \pm 11.4$ | 0.991 |
| $EO_{0.70}PhTFSI_{0.30}$ | $3.40 \times 10^{3}$ | $52.7 \pm 21.8$ | 0.985 |
| $EO_{0.58}PhTFSI_{0.42}$ | $1.52 \times 10^{3}$ | $54.4 \pm 26.8$ | 0.999 |
| $EO_{0.50}PhTFSI_{0.50}$ | $7.53 \times 10^{8}$ | $87.5 \pm 41.3$ | 0.998 |
| $EO_{0.30}PhTFSI_{0.70}$ | $2.66 \times 10^{4}$ | $73.1 \pm 36.1$ | 0.999 |
| Arrhenius Model: $\kappa(T) = \kappa_0 e^{\left(-\frac{Ea}{RT}\right)}$ | | | |

**Table S3.** Vogel-Fulcher-Tammann (VFT) model fitting parameters of $EO_xPhTFSI_y$ blends. Each composition was fit from 70 – 90 °C and $R^2 > 0.98$ for all compositions.

| Sample | $\kappa_0$ (S/cm) | $B$ (K) | $T_0$ (K) | $R^2$ |
|---|---|---|---|---|
| $EO_{0.90}PhTFSI_{0.10}$ | $4.12 \times 10^{-7}$ | 578.4 | 503.2 | 0.980 |
| $EO_{0.70}PhTFSI_{0.30}$ | $1.83 \times 10^{-8}$ | 1261.7 | 511.2 | 0.986 |
| $EO_{0.58}PhTFSI_{0.42}$ | $1.43 \times 10^{-9}$ | 1599.0 | 528.2 | 0.992 |
| $EO_{0.50}PhTFSI_{0.50}$ | $6.04 \times 10^{-12}$ | 3207.7 | 548.3 | 0.998 |

| | | | | |
|---|---|---|---|---|
| $EO_{0.30}PhTFSI_{0.70}$ | $1.03 \times 10^{-14}$ | 4329.3 | 601.2 | 0.996 |
| VFT Model: $\kappa(T) = \kappa_0 e^{\left(-\frac{B}{T-T_0}\right)}$ | | | | |